JARO (2018)
DOI: 10.1007/s10162-018-00690-3

Research Article

JARO
Journal of the Association for Research in Otolaryngology

Otoprotective Effects of *Stephania tetrandra* S. Moore Herb Isolate against Acoustic Trauma

Yan Yu,[1,2] Bing Hu,[2,3,4] Jianxin Bao,[2,5] Jessica Mulvany,[2,5] Eric Bielefeld,[6] Ryan T. Harrison,[6] Sarah A. Neton,[6] Partha Thirumala,[7] Yingying Chen,[2] Debin Lei,[2] Ziyu Qiu,[5] Qingyin Zheng,[3] Jihao Ren,[4] Maria Cristina Perez-Flores,[8] Ebenezer N. Yamoah,[8] and Pezhman Salehi[2]

[1]*The First People's Hospital of Zhangjiagang, 68 W Jiyang Road, Zhangjiagang City, 215600, Jiangsu, China*

[2]*Translational Research Center, Northeast Ohio Medical University, Rootstown, OH 44272, USA*

[3]*Department of Otolaryngology-Head and Neck Surgery, Case Western Reserve University School of Medicine, Cleveland, OH 44106, USA*

[4]*Department of Otolaryngology Head and Neck Surgery, The Second Xiangya Hospital of Central South University, Changsha, 440011, Hunan, China*

[5]*Department of Research and Development, Gateway Biotechnology Inc., Rootstown, OH 44272, USA*

[6]*Department of Speech and Hearing Science, Ohio State University, Columbus, OH 43210, USA*

[7]*The University of Pittsburgh Medical Center, Suite B-400, 200 Lothrop Street, Pittsburgh, PA 15213, USA*

[8]*Department of Physiology and Cell Biology, University of Nevada Reno, 1664 North Virginia St, Reno, NV 89557, USA*

Received: 6 March 2017; Accepted: 8 July 2018

ABSTRACT

Noise is the most common occupational and environmental hazard, and noise-induced hearing loss (NIHL) is the second most common form of sensorineural hearing deficit. Although therapeutics that target the free-radical pathway have shown promise, none of these compounds is currently approved against NIHL by the United States Food and Drug Administration. The present study has demonstrated that tetrandrine (TET), a traditional Chinese medicinal alkaloid and the main chemical isolate of the *Stephania tetrandra* S. Moore herb, significantly attenuated NIHL in CBA/CaJ mice. TET is known to exert antihypertensive and antiarrhythmic effects through the blocking of calcium channels. Whole-cell patch-clamp recording from adult spiral ganglion neurons showed that TET blocked the transient Ca^{2+} current in a dose-dependent manner and the half-blocking concentration was $0.6 + 0.1$ μM. Consistent with previous findings that modulations of calcium-based signaling pathways have both prophylactic and therapeutic effects against neural trauma, NIHL was significantly diminished by TET administration. Importantly, TET has a long-lasting protective effect after noise exposure (48 weeks) in comparison to 2 weeks after noise exposure. The otoprotective effects of TET were achieved mainly by preventing outer hair cell damage and synapse loss between inner hair cells and spiral ganglion neurons. Thus, our data indicate that TET has great potential in the prevention and treatment of NIHL.

Keywords: noise-induced hearing loss, calcium channel, hair cells, spiral ganglion neurons, synapse, *Stephania tetrandra*, TetrandrineYan Yu and Bing Hu contributed equally to this work.

Yan Yu and Bing Hu contributed equally to this work.

Electronic supplementary material The online version of this article (https://doi.org/10.1007/s10162-018-00690-3) contains supplementary material, which is available to authorized users.

Correspondence to: Pezhman Salehi · Translational Research Center · Northeast Ohio Medical University · Rootstown, OH 44272, USA. yueryanzi2003@163.com, yahu1985@126.com

Published online: 05 September 2018

INTRODUCTION

Noise-induced hearing loss (NIHL) is a significant occupational and recreational health issue. Currently, 12.8 % of the American population from 20 to 69 years of age is estimated to have NIHL (Mahboubi et al. 2013). To date, there are no drugs approved by the United States Food and Drug Administration (FDA) to protect against NIHL (Mukherjea et al. 2015), partly due to the complicated cellular and molecular pathways underlying acoustic trauma (Clifford et al. 2016; Kobel et al. 2016; Sha and Schacht 2017). After noise exposure, the auditory brainstem response (ABR) test can be used to detect two phases of hearing loss. These include a temporary threshold shift (TTS), which is greatest immediately after noise exposure, and is gradually reduced within the first 24 h, and permanent threshold shift (PTS), which is measured 2 to 3 weeks after noise exposure (Ryan et al. 2016; Liberman 2016; Liberman and Kujawa 2017). Recent evidence clearly shows that ribbon synapses between the inner hair cells (IHCs) and spiral ganglion neurons (SGNs) are key points of vulnerability in noise injury (Kujawa and Liberman 2006, 2009; Lin et al. 2011; Furman et al. 2013; Fernandez et al. 2015). This injury can ultimately lead to the degeneration of SGNs. Because of the potential prevalence of noise-induced synaptopathy in the US population, pharmaceutical protection from noise should address both hair cell injury (as indicated by PTS), as well as loss of ribbon synapses.

Extensive studies of the interventions for NIHL focus primarily on the free-radical pathway (Kopke et al. 2000; Harris et al. 2006; Bielefeld et al. 2007; Campbell et al. 2007; Le Prell et al. 2007; Shi et al. 2007; Bielefeld et al. 2011). However, most of these interventions are only partially effective in preventing NIHL (Le Le Prell and Bao 2011). Recently, multiple new signaling mechanisms have been discovered that contribute to NIHL (Bao et al. 2013; Han et al. 2015; Chen et al. 2015; Hill et al. 2016). The Chinese medicinal herb *Stephania tetrandra* of the Menispermaceae family has a long safety profile for the treatment of hypertension, edema, rheumatic disorders, circulatory disorders and inflammatory diseases. The herb acts on multiple targets, and its main chemical isolate, tetrandrine (TET), is a bis-benzylisoquinoline alkaloidsoxazole derivative with antihypertensive and vasodilatory effects. Most initial studies on TET focused on its possible action on calcium channels (Wang and Lemos 1995; Wang et al. 2004). TET can inhibit L- and T-type calcium channels in a variety of excitable cells. TET is also a potent blocker of calcium-activated potassium channels (Miller et al. 1985). However, increasing evidence suggests that TET possesses a wide nonselective spectrum of calcium antagonistic actions (Leung et al. 1994). Since disturbance of cellular calcium homeostasis is a common molecular mechanism that leads to neuronal dysfunction and death, *Stephania tetrandra* and TET could be effective otoprotectants against NIHL based on their effects on calcium signaling alone. In addition to its role as a calcium channel blocker, TET exerts antioxidative and anti-inflammatory effects (Jin et al. 2002; Shen et al. 1999; Koh et al. 2003; Fernandes et al. 2006; Chang et al. 1997; Lin et al. 2009), which could possibly make it a more efficacious drug candidate in the treatment of NIHL. Here, we tested the hypothesis that *Stephania tetrandra* herb or TET might have both prophylactic and therapeutic functions against NIHL by acting at multiple points of vulnerability in the cochlea, including outer hair cell (OHC) death and ribbon synaptic loss between IHCs and SGNs.

MATERIALS AND METHODS

Animals

A total of 141 2-month-old CBA/CaJ mice obtained from Jackson Laboratory (Bar Harbor, ME, USA) were used in the experiments. A mix of males and females was used across experiments. Procedures used with mice were approved by the Institutional Animal Care and Use Committee (IACUC) at the Northeast Ohio Medical University.

Herb and Chemicals

Stephania tetrandra herb extract was purchased from Nanjing King Bamboo Biological Technology Co., Ltd. (China). The herbal extract contained approximately 7.81 % TET weight/weight (*w*/*w*). The extract was mixed with the mouse food (1 % of the extract), and food consumption was calculated daily. Tetrandrine (TET, C38H42N2O6, molecular weight 622.75 g/mol) was purchased from Abcam, USA. TET was dissolved in 0.1 N hydrogen chloride (HCl), and the pH was adjusted to 6.5 with 0.1 N sodium hydroxide (NaOH). The control solution was made with HCl and NaOH, and the pH was adjusted to 6.5. Mice were treated by intraperitoneal (i.p.) injection of TET.

High-Performance Liquid Chromatography (HPLC)

The purity of TET herbal extract was tested by Seventh Wave Laboratories (Maryland Heights, MO). Three repeated samples were dissolved and diluted in dimethyl sulfoxide (DMSO), with the final extract concentration being 1 mg/mL. The standard TET

purchased from Sigma (St. Louis, MO) was dissolved and diluted in DMSO to prepare a stock solution. From the stock solution, standards were prepared at 50, 75, 100, 125, and 150 μg/mL in DMSO. Samples were analyzed directly by high-performance liquid chromatography (HPLC) with UV absorbance detection at 254 nm. Mobile phase A was 0.1 % formic acid in water, and mobile phase B was 0.1 % formic acid in acetonitrile. System components were Shimadzu LC-20 AD equipped with SIL-20 AC autosampler and SPD-10AV UV detector and quaternary pump set to 0.25 mL/min, and the column was Thermo BetaSil C18 (2.1 × 250 mm, 5 μM). The correlation coefficient was 0.9983 for UV detection.

Accelerating Rotarod Test

Mice were evaluated on the accelerating rotarod test (San Diego Instruments, Inc., San Diego, CA) to test the effect of TET on motor coordination, grip strength, and balance. The rotating speed was increased at an acceleration rate of 10 rpm/min. The rod stopped at the highest speed of 40 rpm after a total of 240 s. The length of time that each animal was able to stay on the rod was recorded as the latency to fall. The maximum latency was recorded as 240 s. Mice completed two training sessions (6 trials/session, 1-min rest intervals) on the first day in order to acclimate to the test procedure. The mice then completed one testing session on each of the next three consecutive days at the same time and in the same chamber before TET administration. Baseline performance was calculated as the average performance on the 3 days following training. Rotarod performance after TET injection was evaluated in six trials at 1 and 3 h after injection. The mice in the accelerating rotarod test were tested at four doses of TET (60 mg/kg, 120 mg/kg, 180 mg/kg, and 240 mg/kg). Based on the data obtained from single-dose injections, we carried out the same rotarod test for mice that received five TET injections (once per day) at a concentration of 120 mg/kg.

Testing Groups

Based on the results of the rotarod test and a pilot study comparing the effect of three concentrations of TET (80 mg/kg, 100 mg/kg, and 120 mg/kg) on the hearing thresholds of mice, the dose of 120 mg/kg was used for the NIHL study. For testing the herb extract, we fed CBA/CaJ mice with *Stephania tetrandra* S. Moore herbal extract (herb: $n = 7$; controls: $n = 6$) 14 days (7 days before and 7 days post-noise exposure). For TET testing, the mice were randomized into four groups: 5-day TET (120 mg/kg/day) injection group, prevention group, treatment group, and control group. For the 5-day TET injection group, the mice were injected once per day for five consecutive days: beginning 3 days before noise exposure, and ending 2 days after noise exposure. For the prevention group, the mice received a single injection of 120 mg/kg TET 2 h before noise exposure. For the treatment group, mice received a single injection of 120 mg/kg TET immediately after noise exposure. The control group was treated with vehicle injection over the same schedules as the TET groups.

ABR Testing

Mice were anesthetized with 100 mg/kg ketamine and 10 mg/kg xylazine (i.p.) and placed on a thermostatically controlled heating pad in conjunction with a rectal probe (Yellow Springs Instruments Model 73A). Three platinum recording electrodes were inserted subcutaneously posterior to the mouse's right ear pinna (active), at the vertex (upper part of mouse's head, as reference), as well as in the mouse's mid-back close to tail (ground). The acoustical stimulus generation, ABR wave acquisition, equipment control, and data management were performed using a Tucker Davis Technologies (TDT, Alachua, FL) RZ6 Multi I/O processor and BioSigRZ software. A B&K 4135 1/4-in. speaker was placed 10 cm from the right ear of each animal. Tone burst stimuli (5 ms duration, 0.5 ms rise/fall time) were presented 1000 times at 21/s at frequencies of 5, 10, 20, 28, and 40 kHz. Starting level was typically 90 dB SPL, with 5-dB step decreases. Threshold was determined as the lowest sound pressure level that resulted in a detectable and repeatable ABR wave (wave-1 to 5) that could be judged at each frequency using a 5-dB minimum step size. Noise-induced ABR threshold shifts were calculated by the subtraction of pre-exposure thresholds from the post exposure thresholds. Suprathreshold wave-1 amplitudes were measured at the 90-dB SPL stimulus level for each frequency and used for the assembly of frequency-amplitude input-output functions.

Distortion Product Otoacoustic Emissions (DPOAEs)

DPOAE recording was conducted immediately following the ABR test. The primary tones f1 and f2 were generated and shaped using EMAV software (Neely and Liu 1994) and TDT hardware. DPOAEs were recorded in the form of level/frequency functions; f2/f1 was fixed at 1.2, with the level of the f2 (L2) 10 dB less than the f1 level (L1). L2 was fixed at one level, and f2 frequencies were swept from 6 to 40 kHz in 1/10th octave steps. The 2f1-f2 DPOAE amplitude and surrounding noise floor were extracted. The

signal coming from the ear canal was collected by a modified Knowles low-noise microphone and custom preamplifier.

Noise Exposure

Awake mice were exposed two at a time in divided cages within a foam-lined, double-walled soundproof room (Industrial Acoustics). Broadband noise (4–25 kHz) was generated using custom written LabVIEW software and routed through a power amplifier (Crown CDi1000) to a loudspeaker (Selenium D3500Ti-Nd). The overall noise level was measured at the center of the cage using a B&K 4153 1/4-in. microphone connected to a broadband conditioner amplifier (1–100,000 Hz; Bruel & Kjaer Nexus Amplifier) and monitored using custom-written software.

All subjects, including control animals, were exposed to broadband noise (4–25 kHz, 110 dB SPL) for 30 min.

Cochlear Immunostaining Procedure

After the final ABR and DPOAE measurements, the deeply anesthetized mice were transcardially perfused with cold phosphate-buffered saline (PBS) and 4 % paraformaldehyde in 0.1 M phosphate buffer. Then the cochleae were immediately isolated and immersed in the same fixative solution. After fixation for 1–2 h, the cochleae were decalcified in 0.35 M EDTA for 2 days. Each cochlea was microdissected into six pieces following the method described at the cited website (http://www.masseyeandear.org/research/otolaryngology/investigators/laboratories/eaton-peabody-laboratories/epl-histology-resources/video-tutorial-for-cochlear-dissection). A cochlear frequency map was computed based on 3D reconstruction of the sensory epithelium for OHC and presynaptic ribbon count (Muniak et al. 2013). Dissected pieces were dehydrated in 30 % sucrose and frozen in dry ice for 10 min. Thawed samples were washed three times in PBS and preincubated for 1 h in PBS-blocking buffer (0.03 % Triton X-100, 5 % normal horse serum) at room temperature. Cochlear pieces were incubated with primary antibodies to the following: (1) C-terminal binding protein 2 (mouse anti-CtBP2; BD Transduction Labs, used at 1:200), (2) myosin-VIIa (rabbit anti-myosin-VIIa; Proteus Biosciences, used at 1:200) with matching secondary antibodies (Alexa Fluor 488, 546; Life Technologies, USA). Stained cochlear pieces were mounted on slides with Fluoromount-G (SouthernBiotech, USA) medium and cover-slipped.

Image Analysis

The lengths of mouse cochlea pieces were measured, and a cochlear frequency map was computed using a custom plugin to ImageJ provided by this website: http://www.masseyeandear.org/research/ent/eaton-peabody/epl-histology-resources/. Following the frequency map computation, cochlear structures were located to relevant frequency regions (Kujawa and Liberman 2014). Using a confocal microscope (Leica SP8 AOBS), OHC and IHC zones were both imaged at four frequency locations (10, 20, 28, and 40 kHz) with a high-resolution, oil immersion objective microscope (× 80, numerical aperture 1.0) with two digital zooms.

The total number of OHCs was calculated by counting the number of cells in the three rows of OHCs at each frequency region within a 100-μm length of the cochlea. For IHC ribbon synapse quantification, 3D (*x*-*y*-*z*-axis) images were scanned with the 2.0 digital zoom, by a step size of 0.15 μm on the *z*-axis. Displaying spatial staining, images of z-stacks were three-dimensionally produced by Leica Microsystems LAS AF. Each immunostained presynaptic CtBP2 puncta was counted as a ribbon synapse (Kujawa and Liberman 2006). Synaptic ribbons of ten consecutive IHCs distributed within each frequency region were counted. The synaptic ribbons in the normal cochleae were also calculated using the same method to serve as control comparison samples.

Voltage-Clamp Recording

SGNs were isolated from male and female mouse inner ears as described previously (Lv et al. 2010; Lv et al. 2012). Mice were euthanized, and the temporal bones were removed in a solution containing Minimum Essential Medium with Hanks' Balanced Salts (Invitrogen), 0.2 g/L kynurenic acid, 10 mM $MgCl_2$, 2 % fetal bovine serum (FBS; *v*/*v*), and 6 g/L glucose. The spiral ganglia were dissected and split into three equal segments: apical, middle, and basal across the modiolar axis. We used the apical and basal thirds to obtain viable nuronal yield for the experiments (Lv et al. 2010). Additionally, we pooled tissue from three mice into each SGN culture. The apical and basal tissues were digested separately in an enzyme mixture containing collagenase type I (1 mg/ml) and DNase (1 mg/ml) at 37 °C for 20 min. After a series of gentle triturations and centrifugation in 0.45 M sucrose, the cell pellets were reconstituted in 900 ml culture media (Neurobasal-A, supplemented with 2 % B27 (*v*/*v*), 0.5 mM L-glutamine, 100 U/ml penicillin; Invitrogen) and filtered through a 40-μm cell strainer for cell culture. We cultured SGNs for approximately 24–48 h to allow detachment of Schwann cells from neuronal membrane surfaces. We used strict electrophysiologi-

cal criteria, described previously (Lv et al. 2010), to govern the quality of acceptable data. All electrophysiological experiments were performed at room temperature (21–22 °C). Reagents were obtained from Sigma-Aldrich (St. Louis, MO), unless otherwise specified.

Whole-cell voltage-clamp recordings of Ca^{2+} currents were performed using an Axopatch 200B amplifier (Molecular Devices, Sunnyvale, CA). Current traces were amplified, filtered (bandpass 2–10 kHz), and digitized at 5–500 kHz using an analog-to-digital convertor, Digidata 1200 (Molecular Devices) as described earlier (Levic et al. 2007; Rodriguez-Contreras et al. 2008). In Lv et al. (2012), the contribution of the T-type current was described as roughly 20–30 % of the total Ca^{2+} current. We used a similar strategy to isolate the T-type current, and thus, all other calcium channels were suppressed. Electrodes (2–3 M) were pulled from borosilicate glass and the tips were fire-polished. The electrodes contained (in mM): 70 CsCl, 70 N-methyl-D-glucamine (NMDG), 1 $MgCl_2$, 10 Hepes, 2–5 EGTA, 1 $CaCl_2$, and 4 Cs_2ATP, at pH 7.2 with CsOH. The bath solution was continuously perfused (~2–3 ml/min) and contained (in mM): 120 CholineCl, 20 TEACl, 5 4-AP, 0.02 linopirdine, 2 CsCl, 1.8–5 $CaCl_2$, 0.5 $MgCl_2$, 10 Hepes, and 5 D-Glucose, at pH 7.4 with NaOH. In all cases, the Ca^{2+} concentration was adjusted with Mg^{2+}. Inward Ca^{2+} current traces were generated with depolarizing voltage steps from a holding potential of − 100 to − 80 mV and stepped to varying positive potentials (V = 5–10 mV). The capacitative transients were used to estimate the capacitance of the cell, as an indirect measure of cell size. The seal resistance was typically 10–15 GΩ. Currents were measured with capacitance and series resistance compensation (> 90 %), filtered at 2 kHz using an 8-pole Bessel filter, and sampled at 5 kHz. Given that the maximum current recorded was <1 nA, the expected voltage error was < 1.5 mV. The series resistance was monitored during the course of the experiments. The liquid junction potentials were measured (< 3 mV) and corrected.

Whole-cell Ca^{2+} current amplitudes at varying test potentials were measured at peak levels using a peak detection routine. The current magnitude was divided by the cell capacitance (pF) to generate the current density-voltage relationship. The stock solutions of all channel blockers and agonists were made in either double-distilled H_2O or DMSO and stored at − 20 °C. The final concentration of DMSO in the recording bath solution was ~0.0001 %. This concentration of DMSO had no effect on action potentials nor did it alter Ca^{2+} current recordings (data not shown). Ca^{2+} channel blockers nimodipine (L-type), ω-conotoxin GVIA (CTX; N-type), ω-agatoxin IVA (ATX; P/Q-type), ω-theraphotoxin-Hg1a, and rSNX-482 (Alomone Labs, Israel) were bath-applied for whole-cell recordings. In all cases, liquid junction potentials were measured and corrected as described previously (Rodriguez-Contreras and Yamoah 2001).

Statistical Analyses

GraphPad prism version 7.04 was used for statistical analysis. ABR threshold shifts, ABR wave-1 amplitudes, DPOAE amplitudes, OHC counts, and ribbon synapse losses were all analyzed with two-way analyses of variance (ANOVAs). Post hoc comparisons were made using Fisher's LSD multiple comparison tests. Two-tailed, unpaired, Student's t test was used for accelerated rotarod performance. Statistical significance was set at P value ≤ 0.05.

RESULTS

The Purity of the Herbal Extract

Following injection of a TET standard, a single HPLC peak was observed at 12.26 min (Fig. 1a). Following injection of each of three replicates of the herbal extract, three peaks were observed (Fig. 1b). The sources of the first two peaks were unknown (Peak 1, 2); however, the peak eluting at 12.27 min was consistent with TET. The mean TET concentration was 78.1 μg/mg herbal extract.

Herbal Extract of *Stephania tetrandra* S. Moore Ameliorates Noise-Induced Damage

The uptake of TET for the fed group was roughly 60–70 mg/kg/day, which was calculated based on the daily consumption of food containing *Stephania tetrandra* S. Moore (food pellets containing 1 % w/w herbal extract). The results of the herbal extract treatment (Fig. 2) showed no statistical difference between the control (noise, n = 6) and the extract-fed mice (noise + herb, n = 7) 24 h after noise exposure [F (1, 54) = 1.83, P = 0.182]. For the 2-week-post-noise exposure ABR, the two-way ANOVA result for ABR thresholds of mice receiving the herbal extract (n = 7) showed a main effect of group [F (1, 49) = 4.15, P = 0.047] and frequency [F (4, 49) = 7.248, P = 0.001] compared to controls (n = 5). As shown in Fig. 2b, Fisher's LSD post hoc testing revealed reduced threshold shift for TET-treated mice at 10 kHz compared to noise-exposed controls (P = 0.041).

TET Safe Dosage

To determine whether TET was the major contributor of the protection effect against NIHL by *Stephania*

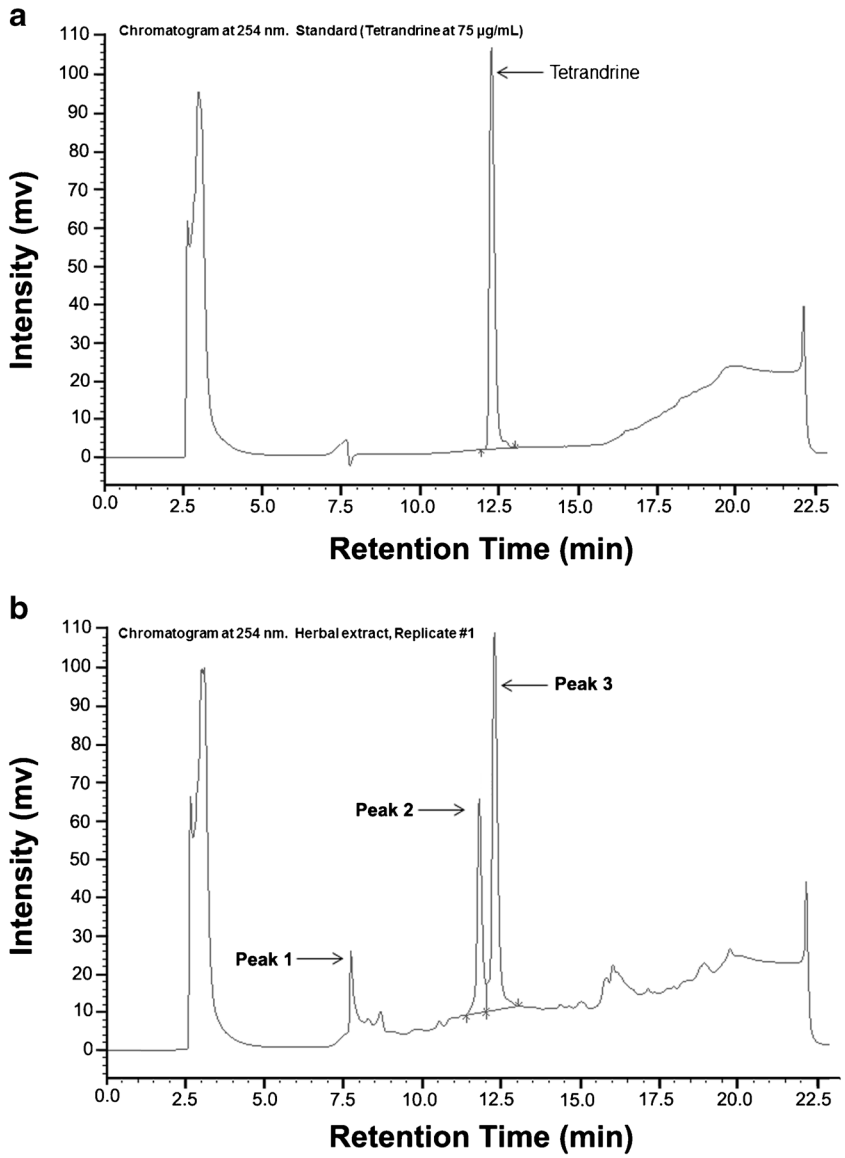

FIG. 1. TET content of the herbal extract. **a** HPLC chromatogram of TET standard (sigma). **b** Chromatogram of the herbal extract from *Stephania tetrandra* S. Moore. The extract test was repeated three times. A single HPLC peak at 12.26 min consistent with TET standard was detected. The mean TET concentration was 78.1 µg/mg herbal extract. All tests were conducted by Seventh Wave Laboratories

tetrandra S. Moore herbal extract, we first determined a safe TET dosage in CBA/CaJ mice with the accelerating rotarod test, which is a standard test for monitoring motor sensory neurotoxicity. The results of the rotarod test (Fig. 3) revealed that single doses of TET at concentrations of 180 mg/kg ($n = 10$) and 240 mg/kg ($n = 7$) significantly reduced the performance at 1-h [180 mg/kg: paired, two-tailed *t*-test, $t(9) = 4$, $P = 0.0008$; 240 mg/kg: $t(5) = 3.561$, $P = 0.0162$] and 3-h [180 mg/kg: paired, two-tailed t test, $t(9) = 3.75$, $P = 0.0045$; 240 mg/kg: $t(5) = 2.79$, $P = 0.0384$] time points after injection compared to baseline measurements. Mice receiving TET dosages of 60 mg/kg and 120 mg/kg showed higher mean latency to fall values when compared to baseline measurements due to repeated testing. However, this improvement was not statistically significant. As shown in Fig. 4, TET repeated injections at 120 mg/kg did not negatively affect the performance of mice after 3 days [paired, two-tailed t test, $t(7) = 0.378$, $P = 0.716$] or 5 days of treatment [paired, two-tailed t test, $t(7) = 0.345$, $P = 0.742$].

TET Diminishes NIHL

Given the rotarod safety results, CBA/CaJ mice were injected with TET at 120 mg/kg once per day for five consecutive days: beginning 3 days before noise exposure, and ending 2 days after noise exposure. Controls received vehicle injections on the same

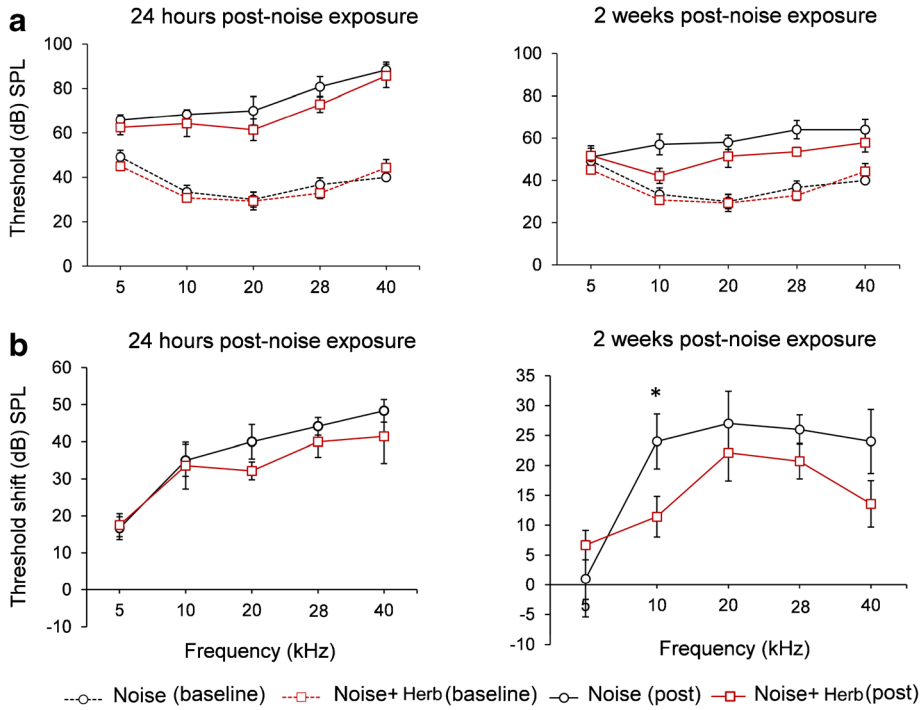

FIG. 2. Noise-induced ABR threshold shift in mice fed with *Stephania tetrandra* S. Moore herbal extract (1 % in the food). **a** Hearing thresholds and **b** threshold shifts showing the effect of herbal extract 24 h and 2 weeks post-noise exposure. Statistical analysis was performed for hearing threshold shifts and showed significant difference between noise and TET/noise group at 10 kHz 2 weeks after noise exposure. Values are means ± SE

schedule. Twenty-four hours after noise exposure, the two-way ANOVA revealed a main effect of group [F (1, 55) = 11.2, P = 0.0015] and frequency [F (4, 55) = 21.5, P = 0.0001] such that TET animals (n = 9) had reduced ABR thresholds when compared to controls (n = 9). Fisher's LSD test showed reduced level of hearing thresholds at 28 kHz for TET-treated mice (P = 0.188) when compared to noise-exposed controls (Fig. 5b). Two weeks after noise exposure, our statistical analysis showed a main effect of group [F (1, 45) = 28.78, P = 0.0001] and frequency [F (4, 45) = 5.01, P = 0.0012] with reduced ABR thresholds for the TET-treated group (n = 9) at 20 kHz (P = 0.0057), 28 kHz (P = 0.005), and 40 kHz (P = 0.0001). At 48 weeks post-noise exposure, our data analysis revealed a main effect of group [F (1, 45) = 19.52, P = 0.0001], frequency [F (4, 55) = 6.909, P = 0.0002], and lower level of ABR thresholds at 28 kHz (P = 0.0005) and 40 kHz (P = 0.0001) for TET-treated mice compared to noise-exposed controls. These results suggested that TET could protect against NIHL. ABR testing of untreated controls did not show any effect of aging on hearing thresholds of CBA/CaJ mice at ages ranging from 2 to 14 months old, (Fig. 8). The effect of TET on NIHL at 12, 24, and 36 weeks post-noise exposure are shown in Fig. S1.

The number of animals at each testing point for the TET/noise group was seven mice at 24 h and 2 weeks post-noise exposure, and five mice at 48 weeks post-noise exposure. For the noise group, six mice at 12 and 24 weeks post-noise exposure, and five mice at 48 weeks post-noise exposure were used. For the no-noise group, 21 mice at 8 weeks old, 32 mice at 4 months old, and 6 mice at 56 weeks old were used. The no-noise mice were matched to the ages of the TET/noise and noise-only mice at 24 h, 2 weeks, and 48 weeks post-noise exposure, respectively.

To directly determine whether TET has both prophylactic and therapeutic effects against NIHL in mice, we administered TET to the CBA/CaJ mice at 120 mg/kg TET in a single dose either 2 h before (prevention group: n = 8) or immediately after (treatment group: n = 7) the noise exposure. The ABR threshold shifts at 24 h and 2 weeks post-noise exposure for the control (n = 5), prevention, and treatment groups are presented in Fig. 6a. For TTS (Fig. 6a), comparison of the noise-exposed group with the prevention and treatment groups were performed separately and revealed a main effect of group [F (1, 60) = 7.157, P = 0.0002] and frequency [F (4, 60) = 13.63, P = 0.0001] for the prevention group comparison, and a main effect of group [F (1, 60) = 24.27, P = 0.0001] and frequency [F (4, 60) = 6.29, P = 0.0003] for the treatment group comparison. Pairwise comparisons of the main effects of group revealed that the prevention and treatment groups had significantly

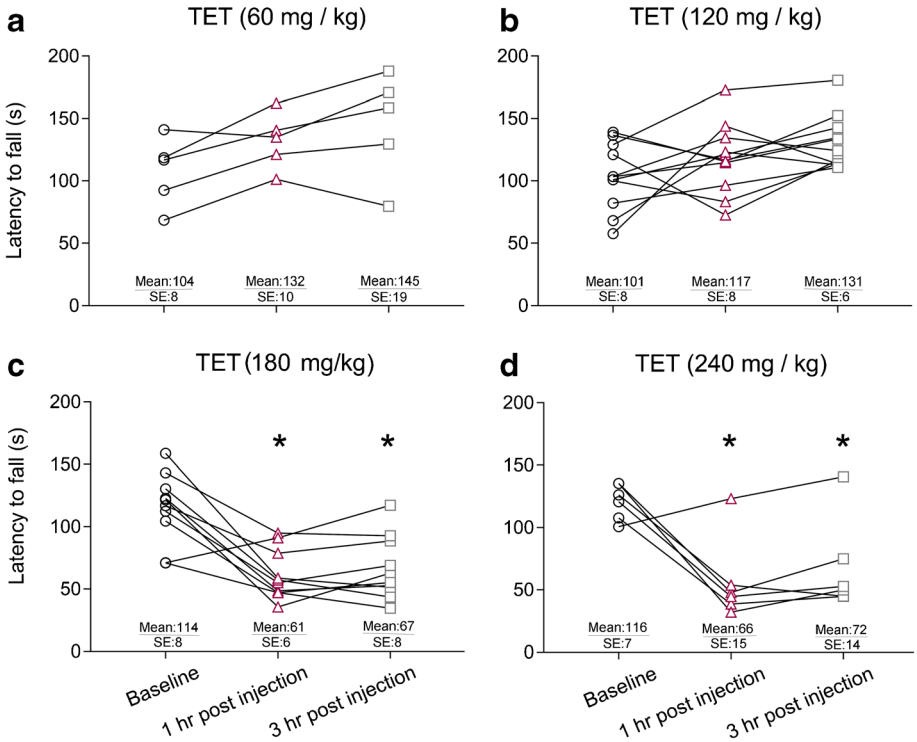

FIG. 3. Accelerating rotarod performance after TET administration. Latencies of the groups with TET at one of the four doses were tested at two time points: 1 h and 3 h after TET application. The number of mice in each group were 7 for the control group, and for the TET groups, 7 mice received 60 mg/kg TET, 12 mice received 120 mg/kg TET, 10 mice received 180 mg/kg TET, and 7 mice received 240 mg/kg TET. **a**, **b** Non-toxic doses of TET: No significant difference between baseline and two other time points for TET concentrations of 60 and 120 mg/kg. **c**, **d** Mean (± SE) values showing significant differences between baseline and 1, and 3 h post-injections for 180 and 240 mg/kg TET concentration (*$P < 0.05$, compared to baseline, *t* test)

lower threshold shifts than the control group at 5 kHz ($P = 0.0007$) and 40 kHz ($P = 0.0011$). For PTS (Fig. 6b), we observed a main effect of group [F (1, 60) = 25.99, $P = 0.0001$] and frequency [F (4, 60) = 6.866, $P = 0.0001$] for comparison of the noise-exposed group and the treatment group. Fisher's LSD test showed the differences at 5 kHz ($P = 0.367$), 20 kHz ($P = 0.0045$), 28 kHz ($P = 0.0104$), and 40 kHz ($P = 0.0226$).

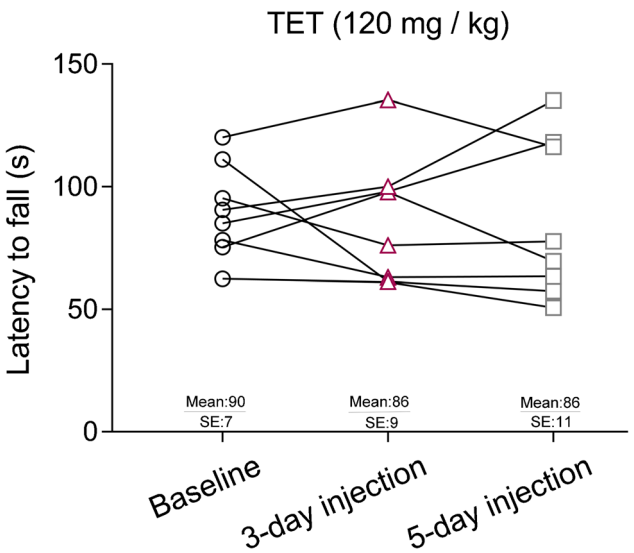

Fig. 4. Accelerating rotarod performance using TET at concentration of 120 mg/kg in CBA/CaJ mice. A mean latency to fall of 86 s after 3 and 5 days TET injection (one injection per day) showed no significant difference between these time points and baseline measurements

DPOAE Changes

To determine whether TET prevented NIHL by protecting OHCs, we measured the DPOAE amplitudes of the CBA/CaJ mice at each f2 frequency (Fig. 7). The control group had DPOAE mean amplitudes lower than the TET-treated group (120 mg/kg; 5-day injection) at 2 weeks and 48 weeks post-noise exposure at several frequencies. The two-way ANOVAs showed a significant effect of group [F (1, 250) = 22.03, $P = 0.0001$] and frequency [F (24, 250) = 8.22, $P = 0.0001$] 2 weeks after noise exposure. Fisher's LSD test for data obtained 2 weeks post-noise showed higher DPOAE amplitudes for the TET-treated group at 26 kHz ($P = 0.0177$), 28 kHz ($P = 0.0035$), 30 kHz ($P = 0.0016$), and 33 kHz ($P = 0.0004$). DPOAE testing at 48 weeks post-noise exposure showed a significant effect of group F (1, 192) = 12.31, $P = 0.0006$], and frequency [F (23, 192) = 6.931, $P = 0.0001$], and higher DPOAE amplitudes at 30 kHz

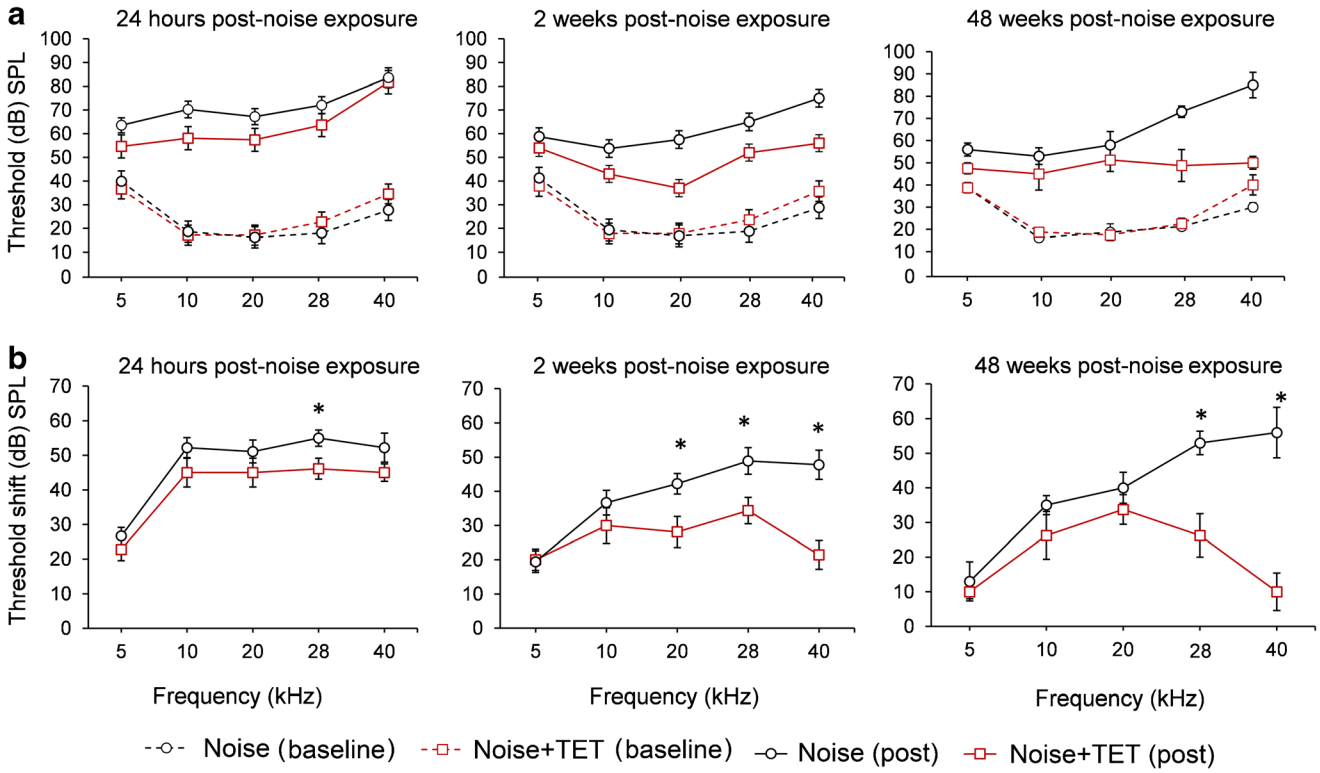

FIG. 5. Noise-induced ABR threshold shift at 24 h, 2 weeks, and 48 weeks post-noise exposure. **a** Hearing thresholds and **b** threshold shifts showing the effect of TET on TTS, 2 weeks, and 48 weeks after noise exposure in CBA/CaJ mice. Values are means ± SE (*$P < 0.05$, compared to baseline, two-way ANOVA)

($P = 0.0136$), and 37 kHz ($P = 0.0021$). A significantly higher level of DPOAE amplitudes of TET-treated mice compared to controls at higher frequencies ranging from 28 to 37 kHz suggests that the protection of OHCs could be one of the cellular mechanisms in which TET prevents NIHL. DPOAE testing of untreated controls did not show any effect of aging on DPOAE amplitudes of CBA/CaJ mice at the ages ranging from 2 to 14 months old (Fig. 8b).

Changes of ABR Wave-1 Amplitudes

We measured mean ABR wave-1 amplitudes at 90 dB suprathreshold for frequencies ranging from 10 to 40 kHz in the control and TET-treated (120 mg/kg, 5-day injection) groups before the noise exposure, and 2 weeks and 48 weeks post-noise exposure (Fig. 9). Two weeks after noise exposure, a two-way repeated measures ANOVA (group x frequency) showed no significant difference between the TET-treated group ($n = 8$) and controls ($n = 5$). Despite this outcome, only animals given TET had ABR wave-1 amplitudes resting above the line of the linear trend (Fig. 9a). ABR wave-1 amplitude at 90 dB analysis 48 weeks after noise exposure (Fig. 9b) showed a main effect of group [F (1, 33) = 19.93, $P = 0.001$] and frequency [F (4, 33) = 7.739, $P = 0.002$] such that TET-treated animals ($n = 4$) had significantly higher wave-1 amplitudes than controls ($n = 5$). Pairwise comparisons demonstrated these differences at 5 kHz ($P = 0.001$) and 28 kHz ($P = 0.0152$).

TET Cellular Targets

To directly assess the cellular mechanisms of TET protection, we performed quantitative immunocytochemical studies. The cochlear samples were immunostained with presynaptic marker CtBP2, one of the most abundant proteins in synaptic ribbon bodies (Sheets et al. 2011). Representative samples of OHCs, IHCs, and ribbon synapses at 40 kHz are displayed in Fig. 10. The numbers of animals were six mice at 2 weeks post-noise exposure for both the TET/noise and noise groups, and four mice for both the TET/noise and noise groups at 48 weeks post-noise exposure. Five untreated mice were used at 2 weeks and 48 weeks post-noise exposure for comparison with noise and TET/noise groups.

At 2 weeks post-noise exposure, the two-way ANOVA did not show a significant difference between untreated controls and the TET/noise group [F (1, 32) = 1.409, $P = 0.2439$]; however, these data showed a

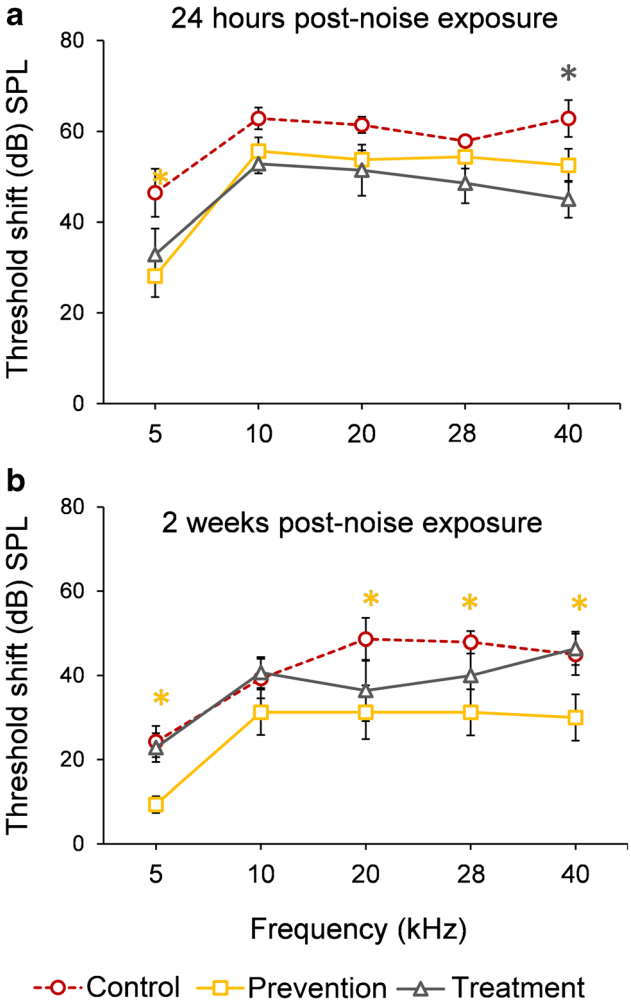

Fig. 6. Prophylactic and therapeutic effects of TET against NIHL. **a** Effect of TET 24 h post-noise exposure. **b** Effect of TET 2 weeks post-noise exposure. Values are means ± SE (*$P<0.05$, compared to baseline, two-way ANOVA)

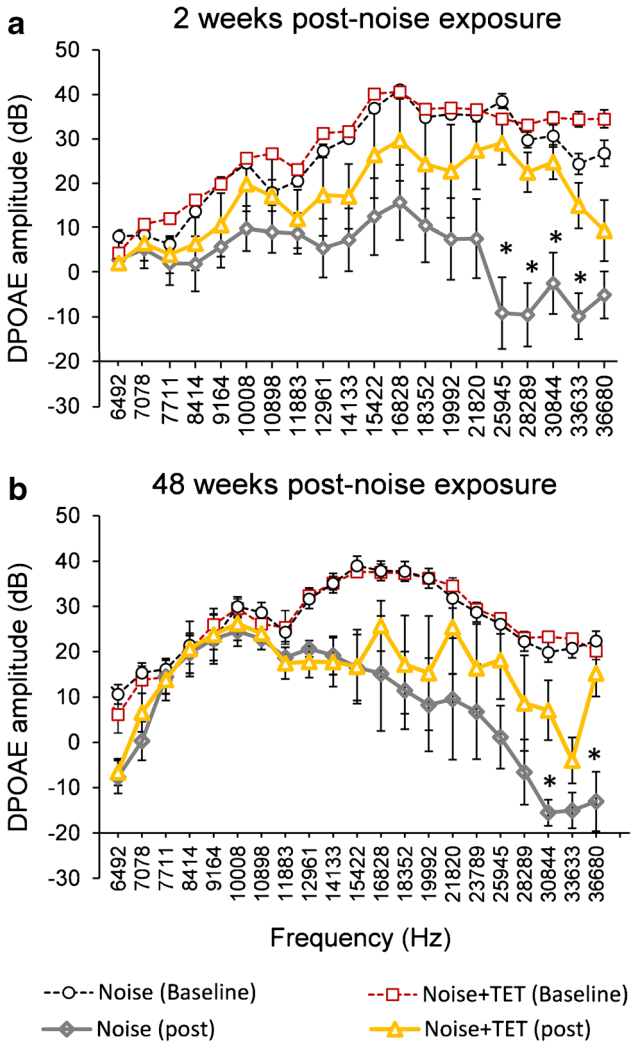

Fig. 7. DPOAE amplitudes of the control and TET groups. **a** Before and 2 weeks after noise exposure in CBA/CaJ mice. **b** Before and 48 weeks after noise exposure in CBA/CaJ mice. Values are means ± SE (*$P<0.05$, compared to baseline, two-way ANOVA)

significant main effect of group for OHC count of the noise-treated group when compared to untreated controls [F (1, 26) = 12.48, P = 0.0016]. Pairwise comparisons demonstrated lower cell counts for the noise-exposed group at 28 kHz (P = 0.0051) when compared to untreated controls (Fig. 10e). At 48 weeks post-noise exposure, statistical analysis again showed a main effect of group when untreated mice were compared to the noise group [F (1, 30) = 48.81, P = 0.0001], with differences at 10 kHz (P = 0.0215), 28 kHz (P = 0.001), and 40 kHz (P = 0.0001). There was no main effect of group between the TET/noise and untreated group [F (1, 28) = 0.2488, P = 0.6218] at 48 weeks post-noise exposure. At 48 weeks post-noise exposure, TET/noise animals had higher counts of OHCs across frequencies compared to the noise-exposed group [F (1, 30) = 48.81, P = 0.001]. Fisher's LSD test showed these differences were significant at 10 kHz (P = 0.0215), 28 kHz (P = 0.001), and 40 kHz (P = 0.0001).

Comparison of the IHC CtBP2 puncta between untreated controls and the noise-exposed group showed a significant main effect of group [F (1, 36) = 226.9, P = 0.001] and frequency [F (3, 36) = 7.461, P = 0.0001] at 2 weeks post-noise exposure. Pairwise comparisons demonstrated this difference at frequency regions of 10 kHz (P = 0.0001), 20 kHz (P = 0.0001), 28 kHz (P = 0.0001), and 40 kHz (P = 0.0001). Untreated controls and the TET/noise group also showed a significant difference between groups [F (1, 32) = 11.78, P = 0.0017] and main effect of frequency [F (3, 32) = 5.355, P = 0.0042] at 2 weeks post-noise exposure. The result of the post hoc test showed significantly higher numbers of IHC CtBP2 puncta in the TET/noise group at 20 kHz (P = 0.0003) and

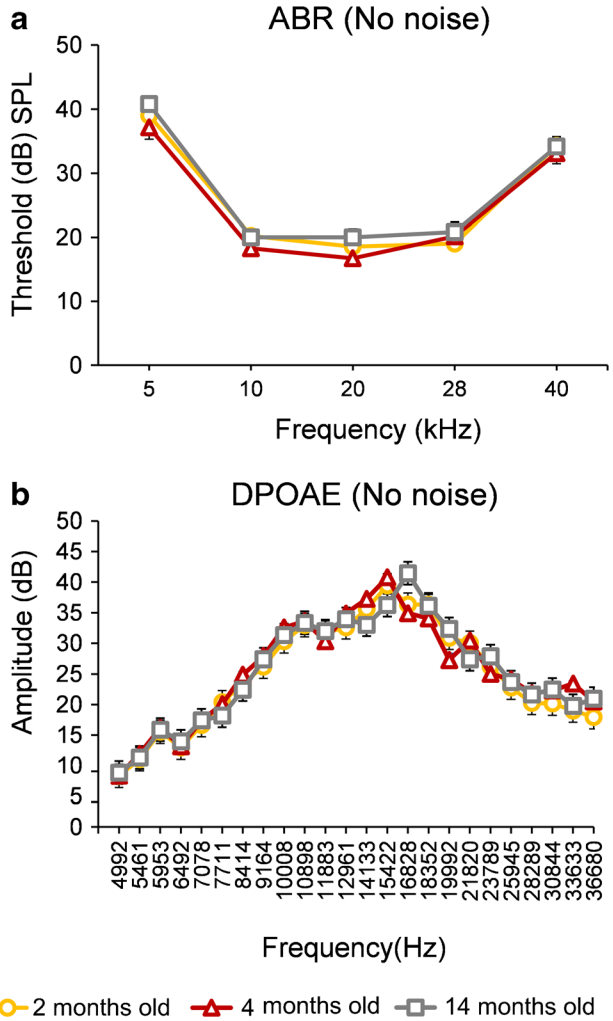

Fig. 8. ABR thresholds and DPOAE amplitudes of non-treated controls. **a**, **b** ABR and DPOAE test of 2, 4, and 14 months old CBA/CaJ mice showed no significant difference between these three age groups. Values are means ± SE

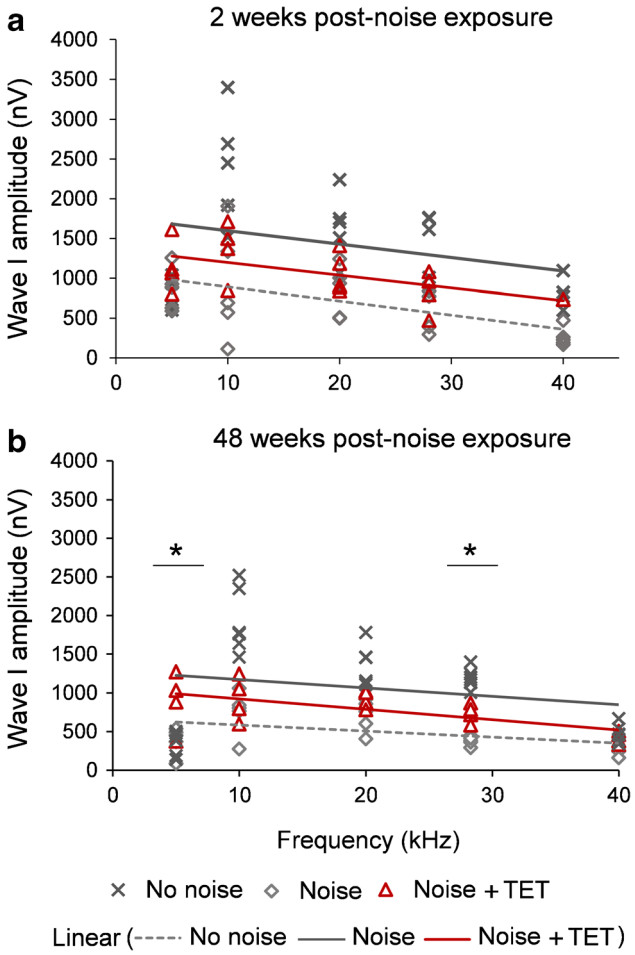

Fig. 9. Mouse ABR wave-1 amplitudes of control and TET groups. ABR wave I amplitudes were calculated at 90 dB suprathreshold for frequencies ranging from 10 to 40 kHz. **a** Data at 2 weeks. **b** Data at 48 weeks after noise exposure. Values are means ± SE

40 kHz ($P = 0.0091$). At 48 weeks post-noise exposure, there was a main effect of group when we compared untreated controls and the noise-exposed group [$F(1,30) = 91.88$, $P = 0.0001$] with differences at frequency regions of 10 kHz ($P = 0.0001$), 20 kHz ($P = 0.0002$), 28 kHz ($P = 0.0001$), and 40 kHz ($P = 0.0001$). Comparison of the untreated controls and the TET/noise group showed a group difference [$F(1, 28) = 9.848$, $P = 0.004$], and the post hoc test showed the difference at 10 kHz region ($P = 0.0189$).

Effects of TET on Transient Ca^{2+} Currents in SGNs

To determine whether one of TET's protection mechanisms was due to TET inhibition of T-type calcium channels on SGNs, we isolated the transient Ca^{2+} current in SGNs using a cocktail of Ca^{2+} current blockers as described previously (Lv et al. 2010; Lv et al. 2012). A cocktail of ω-Agatoxin IVA (ATX) for P/Q-, ω-Conotoxin MVIIA (CTX) for N-, rSNX-482 for R-type, and nimodipine for L- type Ca^{2+} currents, was applied in the bath solution, and the remaining inward Ca^{2+} current traces were elicited from a holding potential of −100 mV to varying depolarizing step voltages (Fig. 11). The sensitivity of the residual current remaining after application of the combined-blocker solution to TET was tested. The current-voltage relationships for two concentrations of TET are shown for eight SGNs isolated from the basal third of the cochlea. TET blocked the transient Ca^{2+} current in a dose-dependent manner, and the half-blocking concentration as determined from six SGNs isolated from one third of the basal region was 0.6 ± 0.1 μM ($n = 6$).

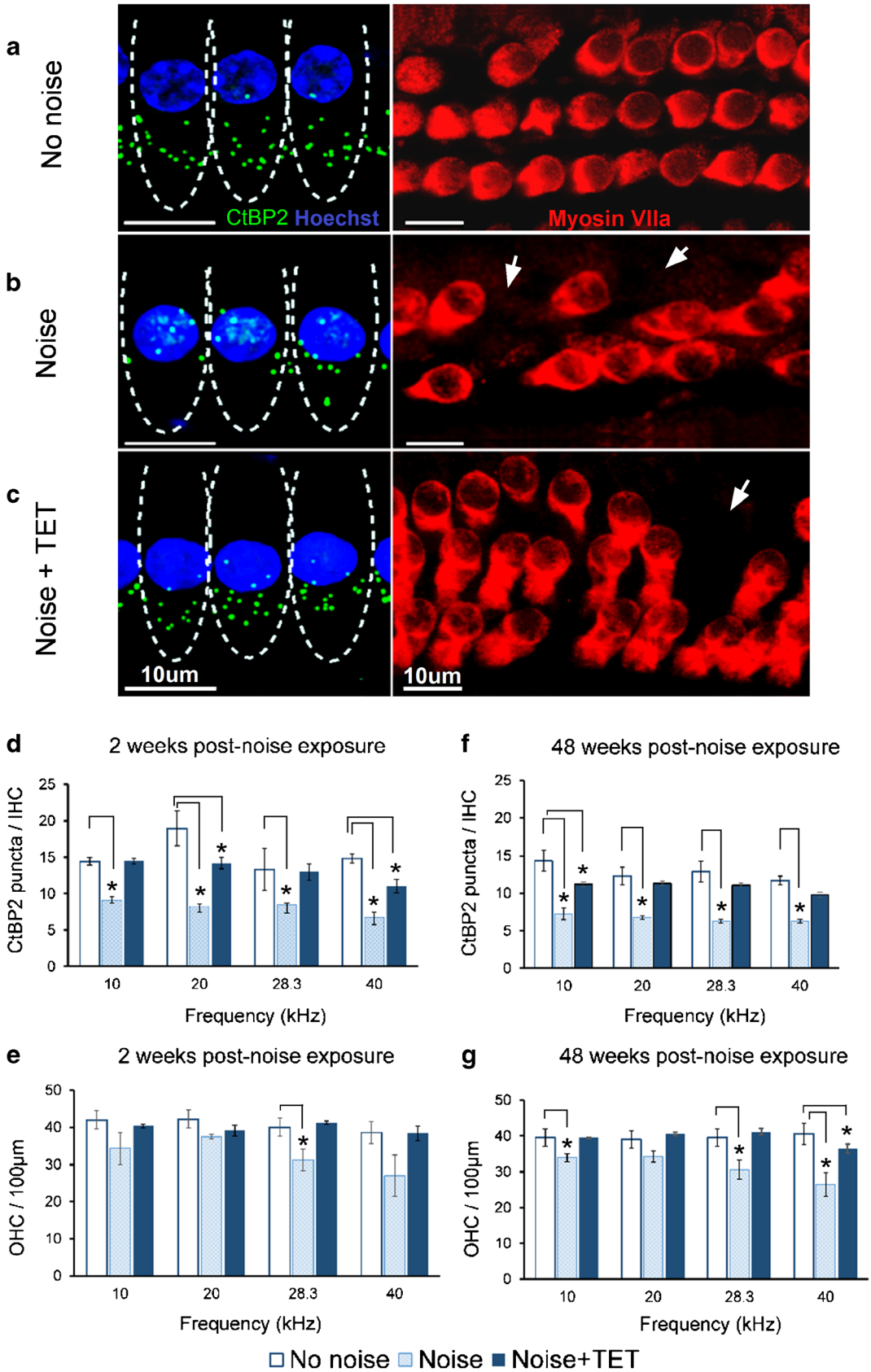

FIG. 10. Protection of IHC ribbon synapses and OHCs by TET. **a** Representative image of IHC ribbon synapses and OHCs at 40 kHz from no noise-exposed cochlea. **b** Noise-exposed cochlea. (**c**) TET-treated cochlea at 2 weeks post-noise exposure. Arrows show missing OHC in TET and control groups. **d-g** Proportions of CtBP2 puncta per IHC and total OHC count per 100 μm were compared between TET/noise, noise, and no noise groups. Values are mean ± SD (*$P < 0.05$, compared to baseline, two-way ANOVA)

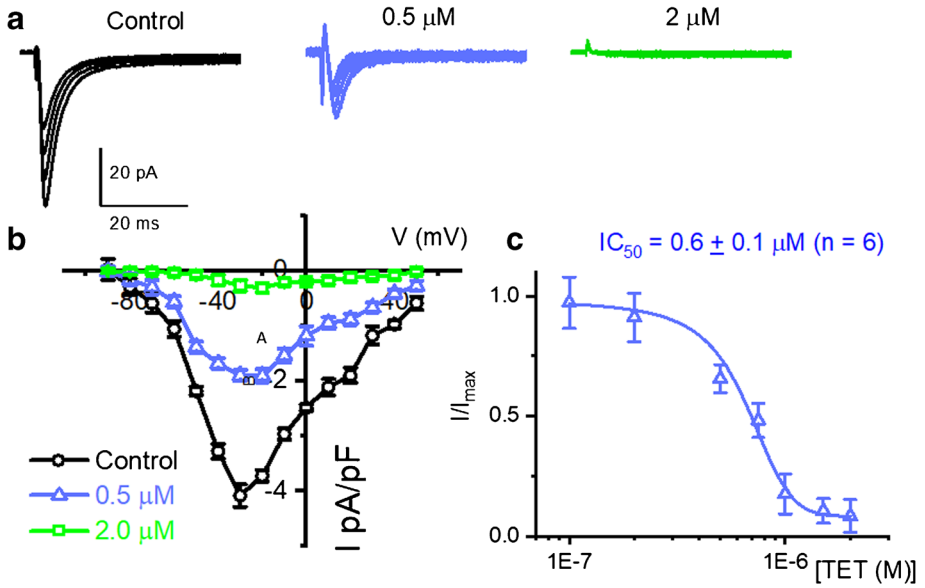

FIG. 11. Whole-cell Ca^{2+} currents in SGNs resistant to a cocktail of L-, N-, P/Q-, and R-type current blockers is sensitive to TET. We used a cocktail of 10 μM nimodipine, 1 μM ω-agatoxin IVA, 1 μM conotoxin MVIIA, and 200 nM rSNX-482. **a** Current traces for control (in black) recorded using a holding voltage of −100 mV to step voltages (in mV, −60, −40, −30, and −10). The middle (in blue) and the right (in magenta) depict the effects of 0.5 M and 2 M TET, respectively on the transient Ca^{2+} current. **b** The corresponding current-voltage relations are shown from data from eight SGNs isolated from the basal one third of the cochlea. **c** The dose-response data was fitted using a Hill equation of the form $I/I_{max} = IC_{50}/(IC_{50} + [TET]^n)$, where IC_{50} = half blocking concentration, and n = Hill's coefficient. The IC_{50} for TET was 0.6 ± 0.1 mM ($n = 6$), and n = 1.2

DISCUSSION

Previously, we reported that a drug combination therapy for NIHL, zonisamide (anticonvulsants) plus methylprednisolone (synthetic glucocorticoids), showed significant synergistic effects against NIHL (Bao et al. 2013). This drug combination study, in addition to other studies, indicates that calcium signaling and inflammatory signaling pathways are both involved in NIHL (Maurer et al. 1998; Tahera et al. 2006). Here, we demonstrate that a single herb extract or the main isolate from this herbal extract, TET, can protect against NIHL by preserving OHCs and the synapses between IHCs and SGNs.

Despite the dramatic effects of TET protection against NIHL at the cellular level, molecular mechanisms underlying this protection are not well understood. Our previous studies suggest a role of calcium signaling in hearing loss (Shen et al. 2007; Wildburger et al. 2009; Bao and Ohlemiller 2010; Perez and Bao 2011; Lei et al. 2011; Kidd Iii and Bao 2012; Bao et al. 2013; Kopecky et al. 2014). Multiple signaling pathways have been implicated in noise-induced cochlear pathology (Abi-Hachem et al. 2010; Gratton et al. 2011; Vetter 2015; Clifford et al. 2016; Groth et al. 2016; Hill et al. 2016). Voltage-gated calcium channels (VGCCs) are strong candidates because Ca^{2+} homeostasis is important for neuronal survival (Clapham 2007; Heyes et al. 2015; Zamponi et al. 2015) and plays a vital role in cochlear function (Levic et al. 2007; Davis and Liu 2011; Lv et al. 2012, 2014). In the cochlea, excitable cells such as hair cells and SGNs express several types of calcium channels, including VGCCs (Rodriguez-Contreras and Yamoah 2001; Adamson et al. 2002; Fuchs 2002; Schnee and Ricci 2003). VGCCs can be divided into two groups: high-voltage activated and low-voltage activated calcium channels (Igelmund et al. 1996; Lacinová et al. 2000; Perez-Reyes 2003; Yunker and McEnery 2003). We have found that NIHL can be ameliorated by anti-convulsant drugs that block low-voltage-activated calcium channels (T-type) (Shen et al. 2007; Bao et al. 2013). T-type calcium channels are known to be present in SGNs (Chen et al. 2011; Lv et al. 2012). In this study, with patch-clamp recording, we have found direct evidence that TET can inhibit T-type calcium channels in adult SGNs. A decrease of calcium influx into the postsynaptic terminal may reduce neuronal excitotoxicity (Kopecky et al. 2014). Thus, this inhibition could be one molecular mechanism underlying TET protection against NIHL, although TET may also act on other mechanisms to protect hearing.

Other in vivo studies provide more evidence regarding the effect of calcium channel blockers on the noise-exposed cochlea, showing that OHCs could be protected during intense noise exposure using the calcium channel blocker diltiazem (Heinrich et al. 1999). Even though the mechanism of protection by calcium blockers is not fully known, Maurer et al.

(1999) have shown that the amount of precipitable calcium increases in the IHCs of noise-exposed cochleae compared to controls. When the antagonist was given before and after acute noise exposure, the calcium content in the IHCs was compared to the amount determined in the untreated group of animals. These data suggest that calcium channel blockers reduce cellular damage caused by excessive calcium levels in noise-exposed cells. Thus, it is also possible that TET could change the Ca^{2+} current in other adult cell types, especially IHCs and OHCs to protect against NIHL.

Detailed functional and histological consequences of NIHL have been established in previous studies (Wang et al. 2002; Kujawa and Liberman 2009; Christie and Eberl 2014). The main cellular damage is synaptic loss between IHCs and SGNs. Based on the intensity and duration of noise, loss of hair cells, especially OHCs, is the second most common form of damage. By using both functional assays and quantitative immunocytochemical methods, we have discovered that TET can diminish noise-induced loss of OHCs and cochlear synapses (between IHCs and SGNs). Based on the current data, it is not clear whether this synaptic protection is a direct or indirect effect due to TET protection of hair cells. In the future, it would be interesting to test whether TET can prevent synapse loss in an NIHL model with only hidden hearing loss, where no loss of hair cells is present.

Regarding the use of the presynaptic marker CtBP2 for the synapse count in this study, the authors are aware that in the normal cochlea, presynaptic ribbons and postsynaptic receptor patches are paired in a way that fewer than 1 % of ribbons are unpaired with a receptor patch (orphan ribbons). The number of orphan ribbons increases after noise exposure. However, at roughly 1 week post-noise exposure, most of the unpaired ribbons paired again with receptor patches (Suzuki et al. 2016). In this study, the presynaptic marker was only used for synapse counts at 2 weeks and 48 weeks post-noise exposure. In the future, it will be necessary to fully characterize the presence of postsynaptic densities or afferent connections to examine the function of TET in promoting functional synapses.

One unexpected finding of this study is a significant TET protection that lasted during aging. Since initial noise damage can lead to accelerated age-related hearing loss (Kujawa and Liberman 2006), these current data strongly suggest that prevention of this initial noise damage could delay accelerated age-related hearing loss caused by early noise exposure. In addition, the clinical implication is that TET can be developed into an effective otoprotective agent, since its protection is preserved during aging.

In conclusion, the present study confirmed that systemic administration of *Stephania tetrandra* S. Moore herb extract (or TET) shows significant protection against NIHL. Based on previous studies, three possible mechanisms underlying this TET otoprotection could be due to its calcium antagonistic actions, antioxidant effects, and anti-inflammatory capability. Here, our patch-clamp data implicates that one mechanism could be due to the blocking of T-type calcium channels in SGNs by TET. Further investigations are needed to determine the relative contributions of other cellular mechanisms. *Stephania tetrandra* S. Moore herb extract and TET have a long-term safety profile in treatment of chronic diseases in Asian countries, which may shorten the duration of time necessary to repurpose them for clinical use against NIHL.

FUNDING INFORMATION

The project was supported by a grant to J. B. from the National Institutes of Health (DC011793, DC016842, and AT008922) and ENY (P01 AG051443, R01DC015135). J.B. is one of the cofounders of Gateway Biotechnology Inc., and has disclosed those interests fully to Northeast Ohio Medical University.

COMPLIANCE WITH ETHICAL STANDARDS

Conflict of Interest The authors declare that they have no conflict of interest.

REFERENCES

Abi-Hachem RN, Zine A, Van De Water TR (2010) The injured cochlea as a target for inflammatory processes, initiation of cell death pathways and application of related otoprotectives strategies. Recent Pat CNS Drug Discov 5:147–163

Adamson CL, Reid MA, Davis RL (2002) Opposite actions of brain-derived neurotrophic factor and neurotrophin-3 on firing features and ion channel composition of murine spiral ganglion neurons. J Neurosci 22:1385–1396

Bao J, Ohlemiller KK (2010) Age-related loss of spiral ganglion neurons. Hear Res 264:93–97

Bao J, Hungerford M, Luxmore R, Ding D, Qiu Z, Lei D, Yang A, Liang R, Ohlemiller KK (2013) Prophylactic and therapeutic functions of drug combinations against noise-induced hearing loss. Hear Res 304:33–40

Bielefeld EC, Kopke RD, Jackson RL, Coleman JK, Liu J, Henderson D (2007) Noise protection with N-acetyl-l-cysteine (NAC) using a variety of noise exposures, NAC doses, and routes of administration. Acta Otolaryngol 127:914–919

Bielefeld EC, Wantuck R, Henderson D (2011) Postexposure treatment with a Src-PTK inhibitor in combination with N-l-acetyl cysteine to reduce noise-induced hearing loss. Noise Health 13:292–298

Campbell KCM, Meech RP, Klemens JJ, Gerberi MT, Dyrstad SSW, Larsen DL, Mitchell DL, El-azizi M, Verhulst SJ, Hughes LF (2007) Prevention of noise- and drug-induced hearing loss with D –methionine. Hear Res 226:92–103

Chang DM, Chang WY, Kuo SY, Chang ML (1997) The effects of traditional antirheumatic herbal medicines on immune response cells. J Rheumatol 3:436–441

Chen WC, Xue HZ, Hsu YL, Liu Q, Patel S, Davis RL (2011) Complex distribution patterns of voltage-gated calcium channel α-subunits in the spiral ganglion. Hear Res 278:52–68

Chen J, Yuan H, Talaska AE, Hill K, Sha SH (2015) Increased sensitivity to noise-induced hearing loss by blockade of endogenous PI3K/Akt signaling. J Assoc Res Otolaryngol 16:347–356

Christie KW, Eberl DF (2014) Noise-induced hearing loss: new animal models. Curr Opin Otolaryngol Head Neck Surg 5:374–383

Clapham DE (2007) Calcium signaling. Cell 131:1047–1058

Clifford RE, Hoffer M, Rogers R (2016) The genomic basis of noise-induced hearing loss: a literature review organized by cellular pathways. Otol Neurotol 37:e309–e316

Davis RL, Liu Q (2011) Complex primary afferents: what the distribution of electrophysiologically-relevant phenotypes within the spiral ganglion tells us about peripheral neural coding. Hear Res 276:34–43

Fernandes MAS, Custódio JBA, Santos MS, Moreno AJM, Vicente JAF (2006) Tetrandrine concentrations not affecting oxidative phosphorylation protect rat liver mitochondria from oxidative stress. Mitochondrion 6:176–185

Fernandez KA, Jeffers PW, Lall K, Liberman MC, Kujawa SG (2015) Aging after noise exposure: acceleration of cochlear synaptopathy in "recovered" ears. J Neurosci 35:7509–7520

Fuchs P (2002) The synaptic physiology of cochlear hair cells. Audiol Neurootol 7:40–44

Furman AC, Kujawa SG, Liberman MC (2013) Noise-induced cochlear neuropathy is selective for fibers with low spontaneous rates. J Neurophysiol 110:577–586

Gratton M, Eleftheriadou A, Garcia J, Verduzco E, Martin GK, Lonsbury-Martin BL et al (2011) Noise-induced changes in gene expression in the cochleae of mice differing in their susceptibility to noise damage. Hear Res 277:211–226

Groth JB, Kao SY, Briët MC, Stankovic KM (2016) Hepatocyte nuclear factor-4 alpha in noise-induced cochlear neuropathy. Dev Neurobiol 76:1374–1386

Han Y, Wang X, Chen J, Sha SH (2015) Noise-induced cochlear F-actin depolymerization is mediated via ROCK2/p-ERM signaling. J Neurochem 133:617–628

Harris KC, Bielefeld E, Hu BH, Henderson D (2006) Increased resistance to free radical damage induced by low-level sound conditioning. Hear Res 213:118–129

Heinrich UR, Maurer J, Mann W (1999) Ultrastructural evidence for protection of the outer hair cells of the inner ear during intense noise exposure by application of the organic calcium channel blocker diltiazem. ORL J Otorhinolaryngol Relat Spec 61:321–327

Heyes S, Pratt WS, Rees E, Dahimene S, Ferron L, Owen MJ, Dolphin AC (2015) Genetic disruption of voltage-gated calcium channels in psychiatric and neurological disorders. Prog Neurobiol 134:36–54

Hill K, Yuan H, Wang X, Sha SH (2016) Noise-induced loss of hair cells and cochlear synaptopathy are mediated by the activation of AMPK. J Neurosci 28:7497–7510

Igelmund P, Zhao YQ, Heinemann U (1996) Effects of T-type, L-type, N-type, P-type, and Q-type calcium channel blockers on stimulus-induced pre- and postsynaptic calcium fluxes in rat hippocampal slices. Exp Brain Res 109:22–32

Jin Q, Kang C, Soh Y, Sohn NW, Lee J, Cho YH, Baik HH, Kang I (2002) Tetrandrine cytotoxicity and its dual effect on oxidative stress-induced apoptosis through modulating cellular redox states in neuro 2a mouse neuroblastoma cells. Life Sci 17:2053–2066

Kidd III AR, Bao J (2012) Recent advances in the study of age-related hearing loss: a mini-review. Gerontology 6:490–496

Kobel M, Le Prell CG, Liu J, Hawks JW, Bao J (2016) Noise-induced cochlear synaptopathy: past findings and future studies. Hear Res 16:30287–30288

Koh SB, Ban JY, Lee BY, Seong YH (2003) Protective effects of fangchinoline and tetrandrine on hydrogen peroxide-induced oxidative neuronal cell damage in cultured rat cerebellar granule cells. Planta Med 6:506–512

Kopecky BJ, Liang R, Bao J (2014) T-type calcium channel blockers as neuroprotective agents. Pflugers Arch 466:757–765

Kopke RD, Weisskopf PA, Boone JL, Jackson RL, Wester DC, Hoffer ME, Lambert DC, Charon CC, Ding DL, McBride D (2000) Reduction of noise-induced hearing loss using L-NAC and salicylate in the chinchilla. Hear Res 149:138–146

Kujawa SG, Liberman MC (2006) Acceleration of age-related hearing loss by early noise exposure: evidence of a misspent youth. J Neurosci 26:2115–2123

Kujawa SG, Liberman MC (2009) Adding insult to injury: Cochlear nerve degeneration after "temporary" noise- induced hearing loss. J Neurosci 45:14077–14085

Kujawa SG, Liberman MC (2014) Synaptopathy in the noise-exposed and aging cochlea: primary neural degeneration in acquired sensorineural hearing loss. Hear Res 330:191–199

Lacinová L, Klugbauer N, Hofmann F (2000) Low voltage activated calcium channels: from genes to function. Gen Physiol Biophys 2:121–136

Le Prell CG, Bao J (2011) Prevention of noise-induced hearing loss: potential therapeutic agents. In: Le Prell CG, Henderson D, Fay RR, Popper AN (eds) Noise-Induced Hearing Loss. Springer Handbook of Auditory Research, vol 40. Springer, New York

Le Prell CG, Yamashita D, Minami SB, Yamasoba T, Miller JM (2007) Mechanisms of noise-induced hearing loss indicate multiple methods of prevention. Hear Res 226:22–43

Lei D, Gao X, Perez P, Ohlemiller KK, Chen CC, Campbell KP, Hood AY, Bao J (2011) Anti-epileptic drugs delay age-related loss of spiral ganglion neurons via T-type calcium channel. Hear Res 278:106–112

Leung YM, Kwan CY, Loh TT (1994) Dual effects of tetrandrine on cytosolic calcium in human leukaemic HL-60 cells: intracellular calcium release and calcium entry blockade. Br J Pharmacol 113:767–774

Levic S, Nie L, Tuteja D, Harvey M, Sokolowski BH, Yamoah EN (2007) Development and regeneration of hair cells share common functional features. Proc Natl Acad Sci U S A 104:19108–19113

Liberman MC (2016) Noise-induced hearing loss: permanent versus temporary threshold shifts and the effects of hair cell versus neuronal degeneration. Adv Exp Med Biol 875:1–7

Liberman MC, Kujawa SG (2017) Cochlear synaptopathy in acquired sensorineural hearing loss: manifestations and mechanisms. Hear Res 16:30250–30257

Lin TY, Tseng SH, Li SJ, Chen JC, Shieh JS, Chen Y (2009) Tetrandrine increased the survival rate of mice with lipopolysaccharide-induced endotoxemia. J Trauma 66:411–417

Lin HW, Furman AC, Kujawa SG, Liberman MC (2011) Primary neural degeneration in the Guinea pig cochlea after reversible noise-induced threshold shift. J Assoc Res Otolaryngol 12:605–616

Lv P, Wei D, Yamoah EN (2010) Kv7-type channel currents in spiral ganglion neurons: involvement in sensorineural hearing loss. J Biol Chem 285:34699–34707

Lv P, Sihn CR, Wang W, Shen H, Kim HJ, Rocha-Sanchez SM, Yamoah EN (2012) Posthearing Ca (2+) currents and their roles in shaping the different modes of firing of spiral ganglion neurons. J Neurosci 32:16314–16330

Lv P, Kim HJ, Lee JH, Sihn CR, Fathabad Gharaie S, Mousavi-Nik A, Wang W, Wang HG, Gratton MA, Doyle KJ, Zhang XD, Chiamvimonvat N, Yamoah EN (2014) Genetic, cellular, and functional evidence for Ca2+ inflow through Cav1.2 and Cav1.3 channels in murine spiral ganglion neurons. J Neurosci 34:7383–7393

Mahboubi H, Zardouz S, Oliaei S et al (2013) Noise-induced hearing threshold shift among US adults and implications for noise-induced hearing loss: National Health and nutrition examination surveys. Euro Arch Otorhinolaryngol 269:839–845

Maurer J, Mann WJ, Amedee RG (1998) Calcium channel blockers for prevention of noise trauma in otologic surgery. J La State Med Soc 150:400–405

Maurer J, Heinrich U, Hinni M, Mann W (1999) Alteration of the calcium content in inner hair cells of the cochlea of the Guinea pig after acute noise trauma with and without application of the organic calcium channel blocker diltiazem. ORL J Otorhinolaryngol Relat Spec 61:328–333

Miller C, Moczydlowski E, Latorre R, Phillips M (1985) Charybdotoxin, a protein inhibitor of single Ca2+–activated K+ channels from mammalian skeletal muscle. Nature 313:316–318

Mukherjea D, Ghosh S, Bhatta P, Sheth S, Tupal S, Borse V, Brozoski T, Sheehan KE, Rybak LP, Ramkumar V (2015) Early investigational drugs for hearing loss. Expert Opin Investig Drugs 24:201–217

Muniak MA, Rivas A, Montey KL, May BJ, Francis HW, Ryugo DK (2013) 3D model of frequency representation in the cochlear nucleus of the CBA/J mouse. J Comp Neurol 7:1510–1532

Neely ST, Liu Z (1994) EMAV: Otoacoustic emission averager, Technical Memo No. 17, Boys Town National Research Hospital, Omaha, NEKLL

Perez P, Bao J (2011) Why do hair cells and spiral ganglion neurons in the cochlea die during aging? Aging Dis 2:231–241

Perez-Reyes E (2003) Molecular physiology of low-voltage-activated t-type calcium channels. Physiol Rev 83:117–161

Rodriguez-Contreras A, Yamoah EN (2001) Direct measurement of single-channel Ca (2+) currents in bullfrog hair cells reveals two distinct channel subtypes. J Physiol 534:669–689

Rodriguez-Contreras A, Lv P, Zhu J, Kim HJ, Yamoah EN (2008) Effects of strontium on the permeation and gating phenotype of calcium channels in hair cells. J Neurophysiol 100:2115–2124

Ryan AF, Kujawa SG, Hammill T, Le Prell C, Kil J (2016) Temporary and permanent noise-induced threshold shifts: a review of basic and clinical observations. Otol Neurotol 37:e271–e275

Schnee ME, Ricci AJ (2003) Biophysical and pharmacological characterization of voltage-gated calcium currents in turtle auditory hair cells. J Physiol 549:697–717

Sha SH, Schacht J (2017) Emerging therapeutic interventions against noise-induced hearing loss. Expert Opin Investig Drugs 26:85–96

Sheets L, Trapani JG, Mo W, Obholzer N, Nicolson T (2011) Ribeye is required for presynaptic Ca(V)1.3a channel localization and afferent innervation of sensory hair cells. Development 7:1309–1319

Shen YC, Chen CF, Wang SY, Sung YJ (1999) Impediment to calcium influx and reactive oxygen production accounts for the inhibition of neutrophil Mac-1 up-regulation and adhesion by tetrandrine. Mol Pharmacol 55:186–193

Shen H, Zhang B, Shin JH, Lei D, Du Y, Gao X, Wang Q, Ohlemiller KK, Piccirillo J, Bao J (2007) Prophylactic and therapeutic functions of T-type calcium blockers against noise-induced hearing loss. Hear Res 226:52–60

Shi X, Han W, Yamamoto H, Omelchenko I, Nuttall A (2007) Nitric oxide and mitochondrial status in noise-induced hearing loss. Free Radic Res 41:1313–1325

Suzuki J, Corfas G, Liberman MC (2016) Round-window delivery of neurotrophin 3 regenerates cochlear synapses after acoustic overexposure. Sci Rep 6:24907

Tahera Y, Meltser I, Johansson P, Hansson AC, Canlon B (2006) Glucocorticoid receptor and nuclear factor-kappa B interactions in restraint stress-mediated protection against acoustic trauma. Endocrinology 147:4430–4437

Vetter DE (2015) Cellular signaling protective against noise-induced hearing loss – a role for novel intrinsic cochlear signaling involving corticotropin-releasing factor? Biochem Pharmacol 97:1–15

Wang G, Lemos JR (1995) Tetrandrine: a new ligand to block voltage-dependent Ca2+ and Ca(+)-activated K+ channels. Life Sci 5:295–306

Wang Y, Hirose K, Liberman MC (2002) Dynamics of noise-induced cellular injury and repair in the mouse cochlea. J Assoc Res Otolaryngol 3:248–268

Wang G, Lemos JR, Iadecola C (2004) Herbal alkaloid tetrandrine: fron an ion channel blocker to inhibitor of tumor proliferation. Trends Pharmacol Sci 25:120–123

Wildburger NC, Lin-Ye A, Baird MA, Lei D, Bao J (2009) Neuroprotective effects of blockers for T-type calcium channels. Mol Neurodegener 4:44

Yunker AM, McEnery MW (2003) Low-voltage-activated ("T-type") calcium channels in review. J Bioenerg Biomembr 35:533–575

Zamponi GW, Striessnig J, Koschak A, Dolphin AC (2015) The physiology, pathology, and pharmacology of voltage-gated calcium channels and their future therapeutic potential. Pharmacol Rev 67:821–870